1 # *Borrelia burgdorferi* DnaA and the nucleoid-associated protein EbfC
2 # coordinate expression of the *dnaX-ebfC* operon

3

4 Andrew C. Krusenstjerna[1], William K. Arnold[1,†], Timothy C. Saylor[1],
5 Jamila S. Tucker[1], and Brian Stevenson[1,2]

6

7 1. Department of Microbiology, Immunology, and Molecular Genetics, University of
8 Kentucky College of Medicine, Lexington, Kentucky, USA
9 2. Department of Entomology, University of Kentucky College of Agriculture, Food, and
10 Ecology, Lexington, Kentucky, USA

11

12 † Current address for W.K. Arnold: ElevateBio LLC, Waltham, Massachusetts, USA

13

14 * For correspondence:
15 Brian Stevenson
16 Department of Microbiology, Immunology, and Molecular Genetics
17 University of Kentucky, College of Medicine
18 Lexington, Ky. 40536-0278
19 Email: brian.stevenson@uky.edu
20 Phone: 1-859-257-9358

ABSTRACT.

Borrelia burgdorferi, the spirochete agent of Lyme disease, has evolved within a consistent infectious cycle between tick and vertebrate hosts. The transmission of the pathogen from tick to vertebrate is characterized by rapid replication and a change in the outer surface protein profile. EbfC, a highly conserved nucleoid-associated protein, binds throughout the borrelial genome affecting expression of many genes, including the Erp outer surface proteins. In *B. burgdorferi*, like many other bacterial species, *ebfC* is co-transcribed with *dnaX*, an essential component of the DNA polymerase III holoenzyme, which facilitates chromosomal replication. The expression of the *dnaX-ebfC* operon is tied to the spirochete's replication rate, but the underlying mechanism for this connection was unknown. In this work, we provide evidence that the expression of *dnaX-ebfC* is controlled by direct interactions of DnaA, the chromosomal replication initiator, and EbfC at the unusually long *dnaX-ebfC* 5' UTR region. Both proteins bind to the 5' UTR DNA, with EbfC also binding to the RNA. The DNA binding of DnaA to this region was similarly impacted by ATP/ADP. *In vitro* studies characterized DnaA as an activator of *dnaX-ebfC* and EbfC as an anti-activator. We further found evidence that DnaA may regulate other genes essential for replication.

37 **IMPORTANCE**

38 The dual-life cycle of *Borrelia burgdorferi*, the causative agent of Lyme disease, is
39 characterized by periods of rapid and slowed replication. The expression patterns of
40 many of the spirochete's virulence factors are impacted by these changes in replication
41 rates. The connection between replication and virulence can be understood at the *dnaX-*
42 *ebfC* operon. DnaX is a component of the DNA polymerase III holoenzyme that facilitates
43 replication. EbfC is a nucleoid-associated protein that regulates the infection-associated
44 outer surface Erp proteins, as well as other transcripts. The expression of *dnaX-ebfC* is tied
45 to replication rate, which we demonstrate is mediated by DnaA, the master chromosomal
46 initiator protein and transcription factor, and EbfC.
47

48 **INTRODUCTION**

49 Replication of the chromosome is a crucial yet costly process. Across all domains of life,
50 chromosomal replication has evolved to require an initiator protein and a replicase (1, 2). For
51 bacteria, the DNA-binding protein DnaA and the DNA polymerase III holoenzyme (DNA Pol III
52 HE) fulfill these roles, respectively. DnaA associates at the chromosomal origin of replication
53 (*oriC*) to high-affinity DnaA-boxes and, through cooperative oligomerization to low-affinity
54 DnaA-boxes, melts the DNA to allow for loading of the helicase and the DNA Pol III HE (3-5).
55 As expected, bacteria have developed distinct pathways to guarantee that this process is initiated
56 appropriately for its environmental conditions.

57 The dual-host enzootic lifecycle of *Borrelia burgdorferi* is intimately tied to replication.
58 This connection is best understood at the tick-vertebrate transmission interface. In the mid-gut of
59 an unfed tick, spirochetes do not replicate, but this changes when the vector takes a blood meal (6-
60 8). Increased nutrient availability permits the spirochetes to replicate their genomes and alter their
61 proteomes to permit the transmission from tick to vertebrate. For *B. burgdorferi*, many of these
62 host-specific phenotypic switches are regulated by a limited repertoire of nucleic acid-binding
63 proteins (9). A notable example is the nucleoid-associated protein EbfC, which directly regulates
64 the production of vertebrate-stage Erp outer surface proteins and numerous other transcripts (10,
65 11).

66 EbfC is highly conserved across eubacteria and is typically the second gene in a bicistronic
67 operon with *dnaX*, an essential component of the DNA Pol III HE (12-14). In the model organism
68 *Escherichia coli*, *dnaX* codes for two subunits, the full-length Tau (τ) and shortened Gamma (γ),
69 by translational frameshift (15-17). All bacterial replicases are composed of three domains
70 essential to their function: a core polymerase, a sliding processivity clamp, and a clamp loading

complex. Tau is the central organizer of these tripartite bacterial replicases, connecting the core polymerases on the leading and lagging strands with the processivity clamp loading complex.

For many bacterial species, DnaA functions as a transcription factor coordinating the expression of genes for various cellular pathways (18, 19). In *B. burgdorferi*, *dnaX-ebfC* transcript levels are tied to bacterial replication rates (20, 21), which we hypothesized could be mediated by DnaA. We found that both DnaA and EbfC contribute to the expression of the *dnaX-ebfC* operon. Additional evidence suggests that DnaA might also be involved with the production of other components of DNA Pol III HE and DNA gyrase.

79 **RESULTS.**

80 **DnaA binds to *dnaX-ebfC* 5' UTR DNA.** Using promoter-reporter fusion constructs, we
81 previously mapped the promoter for the *dnaX-ebfC* operon to be between -247 and -166 bp
82 upstream of the *dnaX* start codon (20). This region is just within the end of the gene for the non-
83 coding signal recognition particle RNA (*srp*; **Fig. 1A**). *In silico* bacterial promoter analysis
84 (BPROM, Softberry; (22)) of this segment of DNA predicted a single σ^{70} promoter, indicating the
85 *B. burgdorferi dnaX-ebfC* operon has a 5' UTR of about 179 nucleotides (**Fig. 1B**). For context,
86 the median 5' UTR in *B. burgdorferi* is ~36 nucleotides in length (23). This significant deviation,
87 in conjunction with the importance of this operon's products to borrelial biology, prompted us to
88 hypothesize that the 5' UTR is critical to *dnaX-ebfC* regulation.

89 As DnaX and EbfC are evidently important for *B. burgdorferi* during periods of rapid
90 replication, we first pursued whether DnaA, which is both the master replication initiator and a
91 transcription factor in other species, can interact with *dnaX-ebfC*. Sequence level examination of
92 the 5' UTR DNA of *dnaX-ebfC* revealed a potential DnaA-box (**Fig. 1B**) (24). To test whether
93 DnaA binds the *dnaX-ebfC* 5' UTR DNA, we performed electrophoretic mobility shift assays
94 (EMSAs) using a recombinant DnaA with a glutathione S-transferase (GST) solubility tag fused
95 to the N-terminus (GST-DnaA).

96 In other bacterial species, the DNA binding activity of DnaA is affected by whether it has
97 ATP or ADP-bound (25-27). As our recombinant GST-DnaA was purified under denaturing
98 conditions and refolded without ATP/ADP, we surmised that the protein adopted an apo-form
99 before use. Thus, our EMSA DNA-binding reactions with GST-DnaA were supplemented with
100 saturating concentrations of either ATP or ADP (**Fig. 2A-B**). Under these conditions, we observed
101 concentration-dependent binding of GST-DnaA to the 186 bp *dnaX-ebfC* 5' UTR DNA probe.

102 Control EMSAs with purified GST confirmed that this binding was not due to the solubility tag
103 (**Fig. 2C**). Quantitative analysis of densitometric data from triplicate EMSAs with GST-DnaA
104 gave overlapping apparent dissociations constants (K_D^{app}) of 1141 nM (95% CI: 703.5-1880 nM)
105 and 737.7 nM (95% CI: 334.8-1639 nM) for ATP and ADP reactions, respectively (**Fig. 2D-F**).
106 These differences were not statistically significant (p = 0.9835, unpaired student's t-test). We
107 concluded that DnaA binds the *dnaX-ebfC* 5' UTR DNA and is not significantly impacted by added
108 ATP/ADP.

109 To narrow down where DnaA is binding in the *dnaX-ebfC* 5' UTR DNA, a competition
110 EMSA with unlabeled competitor DNAs was conducted. The DNA competitors were seven
111 overlapping unlabeled 40-mer sequences from the labeled probe (**Fig. 3A**). The addition of 10-
112 times molar excess of competitors 2 and 3 (C2 & C3), relative to the probe resulted in an
113 appreciable increase in free DNA (**Fig. 3B**, lanes 6 and 7, respectively), indicating preferential
114 binding of the protein to these regions. Competitor 3 contains the hypothesized DnaA-box, but
115 competitor 2 (C2) does not contain a sequence resembling any previously characterized DnaA-
116 box. The inability of the two DNAs that overlap competitor 2 (C5 and C6) to diminish the shifted
117 complex indicates that DnaA bound to a region we term region B (**Fig. 3A**). As a positive control,
118 a specific DNA competitor derived from the pCR2.1 TA clone containing the *dnaX-ebfC* 5' UTR
119 was used. The addition of this DNA resulted in the abrogation of the protein-DNA probe complex
120 (**Fig. 3B**, PC). A negative control, the non-specific DNA derived from the empty pCR2.1 vector,
121 did not affect the protein-probe complex (**Fig. 3B**, NC). These results demonstrate that DnaA binds
122 specifically to regions A and B within the *dnaX-ebfC* 5' UTR DNA.
123

124 **EbfC binds to the *dnaX-ebfC* 5' UTR DNA and RNA.** In addition to the DnaA-boxes
125 identified upstream of the *dnaX* ORF, we also noted two EbfC binding motifs (**Fig. 1A**). EbfC
126 binds with highest affinity to the broken palindromic sequence GTnAC and a lesser affinity to the
127 partial sequence GTnAT (28). EMSAs with recombinant EbfC, nonspecific poly dI-dC competitor,
128 and the 186-mer DNA probe showed specific binding of the protein to this region (**Fig. 4A**).
129 Further EMSAs with 30-mer DNA probes containing either the consensus or partial EbfC motif
130 verified that the EbfC bound each of those sequences (**Fig. 4B-C**). The binding to the complete
131 motif probe was appreciably more prominent than the partial motif probe, consistent with previous
132 characterizations. These results demonstrate that EbfC binds two sites within the *dnaX-ebfC* 5'
133 UTR DNA.

134 During our studies, colleagues shared that EbfC could be pulled down with total RNA from
135 extracts of *B. burgdorferi* (29). We hypothesized that EbfC might also bind the extended *dnaX-*
136 *ebfC* 5' UTR RNA (**Fig. 4D**). To examine this, we performed EMSAs with a 30-mer RNA probe
137 containing the consensus EbfC motif from the *dnaX-ebfC* 5' UTR. Reactions with the RNA probe
138 and recombinant EbfC resulted in the formation of two RNA-protein complexes (**Fig. 4E**, lanes 2-
139 4). The addition of 50-times molar excess of RNA from the constitutively expressed *flaB* did not
140 compete away the complexes (**Fig. 4E**, lane 5). At the same molar excess, the unlabeled *dnaX-*
141 *ebfC* RNA successfully eliminated the smaller complex (**Fig. 4E**, lane 6). These results
142 demonstrated that EbfC can bind untranslated RNA 5' of the *dnaX-ebfC* open reading frames.
143

144 **Assessment of simultaneous binding of DnaA and EbfC to the *dnaX-ebfC* 5' UTR**
145 **DNA.** Having established that DnaA and EbfC bind the 5' UTR DNA of *dnaX-ebfC*, we sought to
146 determine how the proteins would interact in this region. To examine this, EMSA reactions with

147 constant EbfC and increasing GST-DnaA were prepared (**Fig. 5A**). The constant EbfC
148 concentration allowed for roughly equivalent levels of bound and unbound DNA (**Fig. 5A**, lane
149 A). With increasing concentrations of GST-DnaA (**Fig. 5A**, lanes B-G), the DNA-protein complex
150 migrated more slowly in the gel. Densitometry showed an initial increase of free DNAs at low
151 levels of added GST-DnaA (**Fig. 5B**, lanes B-D), followed by a decrease at the highest GST-DnaA
152 concentrations (**Fig. 5B**, lanes E-G). This pattern was not appreciably affected by ATP/ADP.
153 These data suggest that the two proteins may bind cooperatively to the *dnaX-ebfC* 5' UTR DNA.
154 The precise stoichiometry and kinetics of the DNA interactions are undoubtedly complex, given
155 the proximity of the binding sites for each protein.
156
157 **DnaA enhances the expression of *dnaX-ebfC*, while EbfC inhibits this effect.** Having
158 established the interactions of DnaA and EbfC at the *dnaX-ebfC* DNA/RNA, the next logical step
159 was to determine whether the proteins affect the expression of *dnaX-ebfC*. As both proteins are
160 essential for the survival of *B. burgdorferi* (28), analyses with deletion mutant bacteria could not
161 be done. Instead, cell-free *in vitro* transcription/translation assays with *E. coli* S30 extracts were
162 performed. This method has been a useful tool for quantifying DNA-binding proteins' effects on
163 borrelial gene and protein expression and has the added benefit of lacking *B. burgdorferi* DnaA or
164 EbfC (10, 11, 30). The template for these reactions was a linear DNA that contains the 247 bp 5'
165 of *dnaX,* including the transcriptional promoter, fused to *gfp* (20). The addition of GST-DnaA to
166 the *in vitro* reaction resulted in a significant increase ($p = 0.0004$, Brown-Forsythe and Welch
167 ANOVA tests) in the production of the reporter GFP (**Fig. 6**). Control reactions with added GST
168 alone did not significantly change GFP levels.

169 The *in vitro* reactions with recombinant EbfC protein alone did not result in a significant
170 change in GFP output (**Fig. 6**). Only in the presence of GST-DnaA did EbfC exhibit an effect,
171 reducing reporter output to template-only levels (**Fig. 6**). These results indicate that *in vitro*, EbfC
172 alone does not exert a regulatory effect, but it does inhibit the DnaA-dependent activation of *dnaX-*
173 *ebfC* expression. This effect on coupled transcription and translation, combined with the apparent
174 lack of competition between EbfC and DnaA for binding to the 5' UTR DNA (**Fig. 5**), suggests
175 that the effect of EbfC may be through its interaction with RNA.
176
177 **DnaA binds to 5' DNA of other essential replication genes.** The canonical bacterial
178 DNA Pol III HE of *E. coli* consists of nine subunits. Comparatively, the borrelial replicase, like
179 other spirochetes, has a pared-down repertoire (**Table 1**). *B. burgdorferi* has the bare minimum
180 required to replicate its chromosome: a polymerase (DnaE, α), processivity clamp (DnaN, β),
181 clamp loader (DnaX, τ), and clamp opener (HolA, δ). *B. burgdorferi dnaX* does not appear to have
182 the *cis*-element for translational frameshift that produces the Gamma subunit, and so might only
183 produce the Tau subunit (*see* Supplemental material). Moreover, genes for the subunits involved
184 with fidelity (DnaQ, ε; HolE, θ) are absent from the borrelial genome.
185 Since we found that DnaA regulates *dnaX-ebfC*, we posited that DnaA might also be
186 involved in regulating the other subunits of the replicase and itself. With this aim in mind, the 5'
187 intergenic regions of *dnaN*, *dnaE*, *holA,* and *dnaA* were used as labeled DNA probes for EMSA
188 analysis.
189 The *dnaN* gene (BB_0438) codes for the processivity clamp (β) of the DNA Pol III HE
190 and is located downstream of the *dnaA* gene (BB_0437) (**Fig. 7A**). The *B. burgdorferi oriC* is
191 between *dnaA* and *dnaN* and contains two hypothesized DnaA-boxes (31). EMSAs demonstrated

192 the binding of recombinant DnaA to a labeled probe that consisted of the 240 bp *dnaA-dnaN/oriC*
193 region (**Fig. 7B**). The free probe was almost entirely bound by the higher levels of DnaA. There
194 were no appreciable differences in ATP- or ADP-DnaA binding to the *oriC* probe. These results
195 are consistent with the predicted functions of DnaA at *oriC* to control replication initiation.
196 Further, the placement of the *oriC* in proximity to the *dnaN* promoter suggests that DnaA may
197 regulate this gene, as it does in the firmicute *Bacillus subtilis* (32).

198 We also found that DnaA bound the 186 bp 5' intergenic region of *dnaA* and the opposite-
199 facing *gyrB* (BB_0436) (**Fig. 7C**), a location that contains another hypothetical DnaA-box (**Fig.**
200 **7A**) (31). The *gyrB* gene is located upstream of *gyrA* and presumably forms an operon (*gyrBA*) as
201 in other prokaryotes. The *gyrBA* genes code for subunits A and B of the DNA gyrase, a
202 topoisomerase essential in bacterial replication. For the *gyrB-dnaA* region, the free probe was
203 almost entirely bound at the highest protein concentrations. ATP or ADP did not have an
204 appreciable impact on binding to this DNA. These results show that DnaA strongly binds to its
205 promoter region, suggesting it may undergo autoregulation as in other bacteria (25, 32-36).

206 The gene for the DNA polymerase DnaE (α, BB_0579) is located downstream of the gene
207 for a methyl-accepting chemotaxis protein (*mcp-1*, BB_0578) (**Fig. 7A**). The intergenic region
208 between these genes is 130 bp, and it contains a potential DnaA-box (24). EMSAs with
209 recombinant DnaA showed binding to the *dnaE* probe (**Fig. 7D**). ATP/ADP again did not
210 demonstrably affect binding.

211 The *holA* gene (δ, BB_0455) promoter overlaps with a neighboring upstream gene
212 (BB_0454) that codes for a predicted lipid galactosyltransferase (**Fig. 7A**). This intergenic region
213 is small, consisting of only 55 bp, and does not contain a sequence that resembles any known
214 DnaA-box. Despite this, EMSAs showed that DnaA bound to the 5' *holA* DNA (**Fig. 7E**).

215 To compare the relative affinities of DnaA for all these regions, a competition EMSA was
216 performed using the labeled *oriC* DNA as the probe. This DNA was selected as it is the primary
217 site for DnaA interaction and is thus an ideal standard. At 10-times molar excess, the unlabeled
218 DNA competitors from the *dnaX-ebfC* 5' UTR, *dnaE*, and *gyrB-dnaA* considerably depleted the
219 DnaA-*oriC* complex (**Fig. 8**, lanes 5, 6, and 8, respectively). The competitor DNA from *holA*
220 partially diminished the observed shift (**Fig. 8**, lane 7), consistent with the data above (**Fig. 7E**).
221 The negative control DNA derived from the empty pCR2.1 vector, used for all DNAs, failed to
222 compete (**Fig. 8**, lane 9). The unlabeled *oriC* DNA successfully depleted the DnaA-*oriC* probe
223 complex (**Fig 8**, lane 10).

224 With knowledge of the physical interactions of DnaA at these loci, we next sought to track
225 the transcriptional dynamics of these replication genes during the different growth phases of
226 cultured *B. burgdorferi*. As we have established DnaA as an activator of *dnaX-ebfC* transcription
227 *in vitro*, we hypothesized that they would have similar expression profiles. Indeed, the data show
228 that the relative levels of *dnaX* and *ebfC* transcripts rose with *dnaA* as the culture entered the
229 exponential phase (**Fig. 9A-C**). Moreover, *dnaX* and *dnaA* declined as the spirochetes entered the
230 stationary growth phase, while *ebfC* remained stable for some time but eventually decreased. This
231 divergence is consistent with our previous finding that *ebfC* has another promoter within the *dnaX*
232 open reading frame (20).

233 The transcript levels of *dnaN* and *dnaE* also followed the pattern seen with *dnaA* (**Fig. 9D-**
234 **E**). The relative expression level for both genes peaked at mid-exponential and steadily decreased
235 into stationary phase. The *holA* gene, in contrast, exhibited a unique expression profile compared
236 to the other components of the DNA Pol III HE. While the other genes' transcripts decreased during
237 stationary, *holA* transcript levels unexpectedly increased (**Fig. 9F**). Furthermore, the relative

238 abundance of the *holA* transcript was considerably low, never reaching levels greater than that of
239 the housekeeping gene *ftsK*. Those results suggest that at least one additional factor controls levels
240 of *holA* transcript.

241 **DISCUSSION**

242 Tight and coordinated regulation of chromosomal replication is a key biological process.
243 The evolution of such regulatory networks was significant for unicellular organisms, which can
244 inhabit dynamic environments that challenge cellular homeostasis. *B. burgdorferi* has evolved the
245 need to concomitantly modulate DNA replication and gene expression during its consistent cycling
246 between tick vectors and vertebrate hosts. These requirements can be appreciated at the *dnaX-ebfC*
247 locus, where DnaX (Tau) assembles with the DNA Pol III HE to facilitate replication, while EbfC
248 binds at sites throughout the nucleoid and presumably affects chromatin structure. Previously we
249 reported that the expression of *dnaX-ebfC* depends on the replication rate (20, 21), but the question
250 of how remained unanswered. This work indicates that this connection can be explained by direct
251 interactions of DnaA and EbfC at the 5' UTR region of *dnaX-ebfC*.

252 DnaA is well established to be a transcription factor in other bacterial species (19). For *B.*
253 *burgdorferi*, our data show that DnaA binds 5' of the *dnaX-ebfC* operon to enhance gene
254 expression. This is a logical pathway to evolve, given that DnaA and DnaX are directly linked to
255 chromosomal replication. Moreover, this mechanism is perhaps conserved as two DnaA boxes are
256 located upstream of the *E. coli dnaX-ebfC* operon (37).

257 Transcriptional control of bacterial DNA replication machinery through DnaA has also
258 been observed in *Caulobacter crescentus*. A gram-negative aquatic bacterium, *C. crescentus*,
259 exhibits a complex cell cycle defined by asymmetric division into stalked and swarmer progeny
260 where DNA replication is initiated only once per cell cycle (38). In *C. crescentus*, DnaA controls
261 the transcription of two DNA replication genes, the helicase, *dnaB*, and DNA Pol III HE ε-subunit,
262 *dnaQ* (39). There is also evidence of an unknown repressor binding to a conserved promoter motif
263 upstream of *C. crescentus dnaX*, *dnaN*, *dnaA*, *dnaK*, and *gyrB* genes (40). Our work suggests that

264 a similar regulation network may exist in *B. burgdorferi*, where DnaA binds upstream of *dnaX*,
265 *dnaN*, *dnaE*, *holA*, *dnaA*, and *gyrB* (**Fig. 10**). The effect of DnaA on these borrelial genes, aside
266 from *dnaX*, remains to be assessed.

267 The potential global transcriptional effects of DnaA in *B. burgdorferi* begs the question of
268 what controls the master initiator. In other bacteria, the cellular ATP/ADP ratio affects the function
269 of DnaA (25-27). Our data failed to identify a measurable effect of either ATP or ADP on DnaA's
270 binding to any tested sequence. This suggests either *B. burgdorferi* DnaA lacks sensitivity to those
271 nucleotides under the tested conditions or the protein has novel control mechanisms. The latter
272 possibility is especially intriguing due to the lack of protein homologs such as DiaA, Hda, and
273 SeqA that regulate DnaA function/expression in other bacterial species (41-43).

274 The idea of novel DnaA-DNA interactions in *B. burgdorferi* has previously been
275 hypothesized, since the borrelial homolog differs in three of eight amino acid residues in the DNA-
276 binding C-terminus that are conserved in other species (44). In the *E. coli* DnaA, two of the
277 divergent amino acids, T451 and S453, form base-specific hydrogen bonds with DNA (45). This
278 suggests that the DnaA protein of *B. burgdorferi* may recognize unique DNA sequences. Our data
279 showing DnaA binding 5' of *holA* and *dnaX-ebfC* 5' UTR region B, which lack sequence similarity
280 to the characterized DnaA-boxes of other species, points to this possibility. Genome-wide
281 distribution of bound DnaA in *B. burgdorferi* to identify the borrelial DnaA-box sequence is
282 currently under investigation.

283 In addition to the regulatory activity of DnaA, our studies demonstrated that EbfC affects
284 *dnaX-ebfC* expression. That is consistent with previous studies by our group, which found that
285 overexpression of EbfC resulted in a decrease of *dnaX* transcript (20). The present work
286 demonstrates that EbfC regulates *dnaX-ebfC* expression by counteracting DnaA-dependent

287 transcriptional activation. The lack of competition between DnaA and EbfC in binding to the *dnaX-*
288 *ebfC* 5' UTR DNA suggests that EbfC may counteract the effect of DnaA by binding to *dnaX-*
289 *ebfC* mRNA, which could alter secondary structure and affect transcription or translation. Further
290 investigations to tease apart the mechanism of regulation is complicated by the fact that
291 mutagenesis of the *dnaX-ebfC* 5' UTR DNA will affect the structure of the mRNA.

292 The fluctuations from tick and vertebrate hosts have been a constant for *B. burgdorferi* for
293 thousands of years. These divergent biological environments have forced the spirochete to evolve
294 a regulatory network to adapt and endure appropriately. In this study, we provided evidence that
295 *B. burgdorferi* uses its DnaA protein to promote the expression of an operon crucial to its
296 replication and survival. DnaX, the central organizer of the DNA Pol III HE, is essential for
297 chromosomal replication. EbfC affects expression of *dnaX-ebfC*, the vertebrate-stage outer surface
298 Erp proteins, and many other borrelial genes. DnaA activity at *dnaX-ebfC* thus permits coordinated
299 expression of replication machinery and a protein needed for borrelial host infection (**Fig. 10**). *B.*
300 *burgdorferi*. DnaA also binds over the promoter of *bpuR*, an RNA- and DNA-binding protein that,
301 in turn, affects expression levels of Erp and several other borrelial proteins (24). We hypothesize
302 that *B. burgdorferi* DnaA also regulates the production of other proteins involved in replication
303 and infection processes.

304 **METHODS AND MATERIALS.**

305 **Bacterial strains and culture conditions.** All studies utilized derivatives of the *B.*
306 *burgdorferi* type strain, B31, and were cultivated in liquid Barbour-Stoenner-Kelly II (BSK-II)
307 medium (46). For RNA analyses, cultured bacteria were subject to temperature shift wherein
308 spirochetes were grown at 23 ºC to mid-exponential phase (~ 5 x 10^7 cells/ml) and passaged 1:100
309 into fresh BSK-II and incubated at 34 ºC. Stationary phase bacteria were collected from cultures
310 at or above 10^8 cells/ml. Culture cell densities were determined by direct counting in a Petroff-
311 Hauser counting chamber with darkfield microscopy.

312

313 **Recombinant proteins.** EbfC was cloned into pET200 and expressed with an N-terminal
314 6xHis affinity tag. Recombinant EbfC was expressed in *Escherichia coli* Rosetta II cells and
315 purified using MagneHis Particles (Promega) as previously described (24, 47).

316 DnaA was cloned into pET-21a(+) with an N-terminal glutathione S-transferase (GST)
317 moiety by the University of Kentucky Protein Core. A GST tag was selected to enhance the
318 solubility of DnaA, which in other bacteria is known to aggregate into insoluble inclusion bodies
319 (48, 49). Recombinant GST-DnaA protein was expressed in *E. coli* BL21 DE3 cells with 1 mM
320 isopropyl-β-d-thiogalactopyranoside (IPTG) overnight at room temperature. Recombinant GST
321 was expressed in *E. coli* Rosetta II cells containing pGEX-3x. Cells were collected by
322 centrifugation and frozen at -80 ºC.

323 Frozen GST-DnaA expressing cells were resuspended in ice-cold wash/binding buffer (4.2
324 mM Na_2HPO_4, 2 mM KH_2PO_4, 140 mM NaCl, 10 mM KCl) and then supplemented with 5% (v/v)
325 B-PER Bacterial Protein Extraction Reagent (Thermo Scientific) before sonication. The soluble
326 fraction was separated by centrifugation and discarded. The insoluble fraction was retained and

327 processed using mild solubilization per Qi and colleagues (50). Briefly, the insoluble pellet was
328 washed three times with inclusion body wash buffer (20 mM Tris, 300 mM NaCl, 1 mM EDTA,
329 1% Triton X-100, 1 M urea, pH 8.0) followed by two washes with phosphate-buffered saline
330 (PBS), pH 7.4 to remove detergent. The final pellet was resuspended in PBS with 2 M urea and
331 frozen at -20 ºC for at least 12 h. The frozen suspension was then thawed at room temperature and
332 dialyzed at 4 ºC for at least 3 h in 1 L of PBS with 1 M urea, 0.5 M urea, and no urea. The clarified
333 soluble protein suspension was purified using MagneGST Glutathione Particles (Promega)
334 according to manufacturer recommendations. Recombinant GST was purified using the same
335 MagneGST conditions but under standard soluble conditions.

336 Purified proteins were dialyzed against EMSA binding buffer (50 mM Tris-HCl, 50 mM
337 KCl, 1 mM EDTA, 1 mM phenylmethanesulfonyl fluoride [PMSF], 1 mM dithiothreitol [DTT],
338 0.01% Tween-20, 10% glycerol) overnight at 4 ºC and concentrated with 10 kDa MWCO Amicon
339 centrifugal filters (Sigma). Protein concentrations were determined by Bradford assay, and purity
340 was assessed by SDS-PAGE with Coomassie brilliant blue staining. Final protein preparations
341 were stored at -80 ºC in 12 μl working aliquots.

342

343 **TOPO Plasmid Constructs.** For these studies, DNA regions of interest were PCR
344 amplified from *B. burgdorferi* B31 genomic DNA with Taq polymerase and TA cloned into
345 pCR2.1 (Thermo Fisher). Constructs were sequenced to guarantee sequence fidelity.

346

347 **Electrophoretic mobility shift assay (EMSA).** Labeled and unlabeled nucleic acids used
348 are described in the **Supplemental Table**. Oligonucleotides for these assays were synthesized by
349 Integrated DNA Technologies (IDT, Coralville, IA). For use as EMSA probes, DNAs were

350 conjugated with a 5' IRDye800 fluorescent tag, while RNAs had a 5' Alexa Fluor 647 tag. Short
351 DNA probes (< 60 bp) were produced by heating two complementary oligonucleotides to 95 ºC
352 for 5 minutes and gradually cooling them to room temperature. Long DNAs (> 60 bp) were
353 produced by PCR amplification from TA cloned plasmids using M13 Forward and M13 Reverse
354 primers, with a fluor tag on the 5' end of the M13 Reverse. PCR products were treated with
355 exonuclease I (New England BioLabs) to remove residual primers. The reactions were precipitated
356 by adding a 1/10 volume of 3 M sodium acetate and a 2.5 times volume of ice-cold 100% ethanol.
357 Glycogen was added at a final concentration of 1 mg/ml to aid pellet visualization. DNA was
358 pelleted by centrifugation at 4 ºC and washed twice with ice-cold 70% ethanol to remove excess
359 salt. The final DNA pellet was air-dried at room temperature for 15 minutes and resuspended in
360 50 μl of TE buffer. Nucleic acid concentrations were determined spectrophotometrically and
361 diluted to 1 μM. Final DNA probes were stored at -20 ºC in working doses of 12 μl.

362 EMSAs were performed essentially as described previously (11, 51). Briefly, protein-
363 nucleic acid binding reactions were carried out at room temperature for 15 min in EMSA binding
364 buffer using either 100 nM or 20 nM probe. All reactions with GST-DnaA were supplemented
365 with 1 mM $MgCl_2$ and 1 mM of either ATP or ADP and allowed to incubate on ice for 15 min
366 before adding DNA. When appropriate, the non-specific competitor Poly dI dC (Roche) was added
367 to each reaction before the probe at a final concentration of 2.5 ng/μl (52). Competitor nucleic
368 acids were also added to reactions before the labeled probe. Prior to electrophoresis, 6x EMSA
369 loading dye (0.8 mg/ml Orange G, 15 mg/ml Ficol 400) was added to each reaction.
370 Electrophoresis was performed with 6% or 10% Novex TBE gels (Thermo Fisher) or in-house 6%
371 polyacrylamide TBE gels. The in-house polyacrylamide TBE gels (40 ml) for horizontal
372 electrophoresis were produced by combining 6 ml 40% Acryl/Bis 29:1 (VWR), 4 ml of 5x TBE,

373 pH 7.5 (445 mM Tris, 445 mM boric acid, 5 mM EDTA), 30 ml ddH_2O, 300 μl 10% APS (Fisher),
374 and 100 μl of TEMED (National Diagnostic). The gels were pre-run in 0.5x TBE buffer at 12.5
375 V/cm for 30 min. Samples were loaded and resolved at 12.5 V/cm until the dye front reached the
376 bottom of the gel.

377 The apparent K_D of GST-DnaA for the *dnaX-ebfC* 5' UTR DNA probe was determined by
378 densitometry from triplicate EMSAs using ImageLab software (BioRad). Lanes were manually set
379 to the EMSA gel. The free DNA and shifted bands were manually selected, and the intensities
380 were reported as lane %. These values were subsequently plotted against the corresponding protein
381 concentration. The plotted data was then subjected to nonlinear regression analysis using Prism 9
382 software. An unpaired t-test was performed to assess statistically significant differences ($\alpha = 0.5$)
383 between the ATP and ADP data.

384

385 **Coupled *in vitro* transcription/translation assays.** Coupled *in vitro*
386 transcription/translation assays were performed as previously described (10, 11, 30). Linear DNA
387 template was amplified from pAAB206 using M13 forward and reverse primers (20). This
388 amplicon contains 247 bp 5' of *dnaX-ebfC* fused to *gfp*. Experiments were performed using the *E.*
389 *coli* S30 Extract System for Linear Templates (Promega). The 50-μl reactions were composed of
390 kit components, 2,100 ng of template DNA (~65 nM), 40 U of RiboGuard RNase Inhibitor
391 (Lucigen), and 1 μM of the proteins of interest, when appropriate. Purified GST was used as a
392 control. Reactions were incubated at 37 ºC for 2 h and promptly iced for 5 minutes to stop
393 transcription/translation. Each reaction set was performed in triplicate.

394 The *in vitro* protein products were precipitated by adding 4-volumes of ice-cold acetone
395 and incubating at -20 ºC for at least one hour. Proteins were pelleted by centrifugation and air-

396 dried on ice for 15 minutes. Dried protein pellets were then resuspended in 100 μl of PBS. Protein
397 suspensions were mixed with 500 μl of ELISA coating buffer (50 mM Na_2CO_3, 500 mM $NaHCO_3$,
398 pH 9.2), and 150 μl of this mixture was added to the wells of 96-well microtiter plates. GFP was
399 detected with MACS anti-GFP-HRP (Militenyi Biotec). Seventy-five microliters of tetramethyl
400 benzidine (TMB; Thermo Scientific) HRP substrate were added to each well and incubated at room
401 temperature with shaking for 30 minutes. Reactions were quenched with 75 μl of 2N H_2SO_4, and
402 the absorbance at 450 nm was measured using a Biotek Epoch 2 microplate reader.
403 Statistical significance (α = 0.05) was determined using Brown-Forsythe and Welch
404 ANOVA tests and Dunnett's T3 multiple comparisons.
405
406 **Quantitative reverse transcription-PCR (qRT-PCR).** To measure the levels of target
407 transcripts, *B. burgdorferi* was cultured at 35 ºC, and 2 ml aliquots of bacteria were taken 1-, 3-,
408 5-, 7-, 9-, and 11-days post-inoculation. Cells were washed two times with PBS and frozen at -80
409 ºC. Frozen pellets were later resuspended in 60 ºC TRIzol (Thermo Fisher), and RNA was
410 extracted using a Qiagen Mini RNA kit. Residual genomic DNA was depleted using on-column
411 Turbo DNase (Thermo Fisher). The quality (RIN > 7) and quantity of the RNA were determined
412 using an Agilent 2100 Bioanalyzer and Agilent 6000 Nano chips. Purified RNA stocks were stored
413 at -80 ºC.
414 Complementary DNA (cDNA) for qPCR was produced using the iScript gDNA Clear
415 cDNA synthesis kit (Bio-Rad). The cDNA stocks were diluted 1:100 into nuclease-free water for
416 use as template. Quantitative PCR was carried out using iTaq Universal SYBR Green Supermix
417 (Bio-Rad) and a Bio-Rad CFX96 Touch Real-time PCR thermocycler. Oligonucleotide primer sets
418 for target genes were designed using the IDT Primer Quest Tool

419 (https://www.idtdna.com/PrimerQuest/Home/Index). For all reactions, cycles involved melting at
420 95 ºC for 10s, annealing at 55 ºC for 10 s, and extension at 72 ºC for 30s. Each run was performed
421 with technical triplicates of each reaction as well as no template control reactions that lacked
422 template. Melting curves were performed with each run to validate the production of specific
423 amplicons. Every reaction was tested with a reverse transcriptase-negative template to validate the
424 absence of contaminating gDNA. Cq values were normalized to *ftsK*, a gene whose expression is
425 stable across different growth phases (53), using the ΔCq method, and fold-difference was
426 determined by the function $2^{-\Delta Cq}$.
427

428 **Acknowledgments**

429 This research was funded by NIH grant R21 AI147139-02. We thank Tatiana Castro-Padovani and
430 Nerina Jusufovic for their helpful comments and support on these studies and the manuscript. The
431 construct for recombinant GST-DnaA was synthesized by Drs. Martin Chow and Lou Hersh of the
432 University of Kentucky COBRE Protein Core. Dr. Tony Sinai kindly provided pGEX-3x.
433 Schematic figures were made using BioRender.

434 **Works Cited.**

435 1. Kawakami H, Katayama T. 2010. DnaA, ORC, and Cdc6: similarity beyond the domains
436 of life and diversity. Biochem Cell Biol 88:49-62.
437 2. McHenry CS. 2011. DNA replicases from a bacterial perspective. Annu Rev Biochem
438 80:403-36.
439 3. Speck C, Messer W. 2001. Mechanism of origin unwinding: sequential binding of DnaA
440 to double- and single-stranded DNA. EMBO J 20:1469-76.
441 4. Kaur G, Vora MP, Czerwonka CA, Rozgaja TA, Grimwade JE, Leonard AC. 2014.
442 Building the bacterial orisome: high-affinity DnaA recognition plays a role in setting the
443 conformation of *oriC* DNA. Mol Microbiol 91:1148-63.
444 5. Ozaki S, Katayama T. 2012. Highly organized DnaA-*oriC* complexes recruit the single-
445 stranded DNA for replication initiation. Nucleic Acids Res 40:1648-65.
446 6. Dunham-Ems SM, Caimano MJ, Pal U, Wolgemuth CW, Eggers CH, Balic A, Radolf JD.
447 2009. Live imaging reveals a biphasic mode of dissemination of *Borrelia burgdorferi*
448 within ticks. J Clin Invest 119:3652-65.
449 7. Piesman J, Oliver JR, Sinsky RJ. 1990. Growth kinetics of the Lyme disease spirochete
450 (*Borrelia burgdorferi*) in vector ticks (*Ixodes dammini*). Am J Trop Med Hyg 42:352-7.
451 8. De Silva AM, Fikrig E. 1995. Growth and migration of *Borrelia burgdorferi* in *Ixodes* ticks
452 during blood feeding. Am J Trop Med Hyg 53:397-404.
453 9. Stevenson B, Seshu J. 2018. Regulation of Gene and Protein Expression in the Lyme
454 Disease Spirochete. Curr Top Microbiol Immunol 415:83-112.
455 10. Jutras BL, Verma A, Adams CA, Brissette CA, Burns LH, Whetstine CR, Bowman A,
456 Chenail AM, Zuckert WR, Stevenson B. 2012. BpaB and EbfC DNA-binding proteins

457 regulate production of the Lyme disease spirochete's infection-associated Erp surface
458 proteins. J Bacteriol 194:778-86.
459 11. Jutras BL, Chenail AM, Carroll DW, Miller MC, Zhu H, Bowman A, Stevenson B. 2013.
460 Bpur, the Lyme disease spirochete's PUR domain protein: identification as a transcriptional
461 modulator and characterization of nucleic acid interactions. J Biol Chem 288:26220-34.
462 12. Blinkova A, Hervas C, Stukenberg PT, Onrust R, O'Donnell ME, Walker JR. 1993. The
463 *Escherichia coli* DNA polymerase III holoenzyme contains both products of the *dnaX*
464 gene, tau and gamma, but only tau is essential. J Bacteriol 175:6018-27.
465 13. Dallmann HG, Thimmig RL, McHenry CS. 1995. DnaX complex of *Escherichia coli* DNA
466 polymerase III holoenzyme. Central role of tau in initiation complex assembly and in
467 determining the functional asymmetry of holoenzyme. J Biol Chem 270:29555-62.
468 14. Cordeiro TFVB, Gontijo MTP, Jorge GP, Brocchi M. 2022. EbfC/YbaB: A Widely
469 Distributed Nucleoid-Associated Protein in Prokaryotes. Microorganisms 10:1945.
470 15. Tsuchihashi Z. 1991. Translational frameshifting in the *Escherichia coli dnaX* gene *in*
471 *vitro*. Nucleic Acids Res 19:2457-62.
472 16. Tsuchihashi Z, Brown PO. 1992. Sequence requirements for efficient translational
473 frameshifting in the *Escherichia coli dnaX* gene and the role of an unstable interaction
474 between tRNA(Lys) and an AAG lysine codon. Genes Dev 6:511-9.
475 17. Larsen B, Gesteland RF, Atkins JF. 1997. Structural probing and mutagenic analysis of the
476 stem-loop required for *Escherichia coli dnaX* ribosomal frameshifting: programmed
477 efficiency of 50%. J Mol Biol 271:47-60.
478 18. Messer W, Weigel C. 1997. DnaA initiator--also a transcription factor. Mol Microbiol
479 24:1-6.

480 19. Menikpurage IP, Woo K, Mera PE. 2021. Transcriptional Activity of the Bacterial
481 Replication Initiator DnaA. Front Microbiol 12:662317.
482 20. Jutras BL, Bowman A, Brissette CA, Adams CA, Verma A, Chenail AM, Stevenson B.
483 2012. EbfC (YbaB) is a new type of bacterial nucleoid-associated protein and a global
484 regulator of gene expression in the Lyme disease spirochete. J Bacteriol 194:3395-406.
485 21. Jutras BL, Chenail AM, Stevenson B. 2013. Changes in bacterial growth rate govern
486 expression of the *Borrelia burgdorferi* OspC and Erp infection-associated surface proteins.
487 J Bacteriol 195:757-64.
488 22. Solovyev V, Salamov A, Li R. 2011. Metagenomics and its applications in agriculture,
489 biomedicine and environmental studies. Autom Annot Microb Genomes Metagenomic Seq
490 Nova Science.
491 23. Adams PP, Flores Avile C, Popitsch N, Bilusic I, Schroeder R, Lybecker M, Jewett MW.
492 2017. *In vivo* expression technology and 5' end mapping of the *Borrelia burgdorferi*
493 transcriptome identify novel RNAs expressed during mammalian infection. Nucleic Acids
494 Res 45:775-792.
495 24. Jutras BL, Savage CR, Arnold WK, Lethbridge KG, Carroll DW, Tilly K, Bestor A, Zhu
496 H, Seshu J, Zuckert WR, Stewart PE, Rosa PA, Brissette CA, Stevenson B. 2019. The
497 Lyme disease spirochete's BpuR DNA/RNA-binding protein is differentially expressed
498 during the mammal-tick infectious cycle, which affects translation of the SodA superoxide
499 dismutase. Mol Microbiol 112:973-991.
500 25. Speck C, Weigel C, Messer W. 1999. ATP- and ADP-*dnaA* protein, a molecular switch in
501 gene regulation. EMBO J 18:6169-76.

502 26. Smith JL, Grossman AD. 2015. *In Vitro* Whole Genome DNA Binding Analysis of the
503 Bacterial Replication Initiator and Transcription Factor DnaA. PLoS Genet 11:e1005258.
504 27. Sekimizu K, Bramhill D, Kornberg A. 1987. ATP activates *dnaA* protein in initiating
505 replication of plasmids bearing the origin of the *E. coli* chromosome. Cell 50:259-65.
506 28. Riley SP, Bykowski T, Cooley AE, Burns LH, Babb K, Brissette CA, Bowman A, Rotondi
507 M, Miller MC, DeMoll E, Lim K, Fried MG, Stevenson B. 2009. *Borrelia burgdorferi*
508 EbfC defines a newly-identified, widespread family of bacterial DNA-binding proteins.
509 Nucleic Acids Res 37:1973-83.
510 29. Van Gundy T, Lybecker M. Identification of RNA chaperones by gradient profiling in the
511 Lyme disease spirochete.
512 30. Jutras BL, Jones GS, Verma A, Brown NA, Antonicello AD, Chenail AM, Stevenson B.
513 2013. Posttranscriptional self-regulation by the Lyme disease bacterium's BpuR
514 DNA/RNA-binding protein. J Bacteriol 195:4915-23.
515 31. Picardeau M, Lobry JR, Hinnebusch BJ. 1999. Physical mapping of an origin of
516 bidirectional replication at the centre of the *Borrelia burgdorferi* linear chromosome. Mol
517 Microbiol 32:437-45.
518 32. Ogura Y, Imai Y, Ogasawara N, Moriya S. 2001. Autoregulation of the *dnaA-dnaN* operon
519 and effects of DnaA protein levels on replication initiation in *Bacillus subtilis*. J Bacteriol
520 183:3833-41.
521 33. Berenstein D, Olesen K, Speck C, Skovgaard O. 2002. Genetic organization of the *Vibrio*
522 *harveyi* DnaA gene region and analysis of the function of the *V. harveyi* DnaA protein in
523 *Escherichia coli*. J Bacteriol 184:2533-8.

524 34. Salazar L, Guerrero E, Casart Y, Turcios L, Bartoli F. 2003. Transcription analysis of the
525 *dnaA* gene and *oriC* region of the chromosome of *Mycobacterium smegmatis* and
526 *Mycobacterium bovis* BCG, and its regulation by the DnaA protein. Microbiology
527 (Reading) 149:773-784.
528 35. Jakimowicz D, Majka J, Lis B, Konopa G, Wegrzyn G, Messer W, Schrempf H,
529 Zakrzewska-Czerwinska J. 2000. Structure and regulation of the *dnaA* promoter region in
530 three *Streptomyces* species. Mol Gen Genet 262:1093-102.
531 36. Atlung T, Clausen E, Hansen FG. 1984. Autorepression of the *dnaA* gene of *Escherichia*
532 *coli*. Adv Exp Med Biol 179:199-207.
533 37. Flower AM, McHenry CS. 1986. The adjacent *dnaZ* and *dnaX* genes of *Escherichia coli*
534 are contained within one continuous open reading frame. Nucleic Acids Res 14:8091-101.
535 38. Collier J. 2019. Cell division control in *Caulobacter crescentus*. Biochim Biophys Acta
536 Gene Regul Mech 1862:685-690.
537 39. Hottes AK, Shapiro L, McAdams HH. 2005. DnaA coordinates replication initiation and
538 cell cycle transcription in *Caulobacter crescentus*. Mol Microbiol 58:1340-53.
539 40. Keiler KC, Shapiro L. 2001. Conserved promoter motif is required for cell cycle timing of
540 *dnaX* transcription in *Caulobacter*. J Bacteriol 183:4860-5.
541 41. Ishida T, Akimitsu N, Kashioka T, Hatano M, Kubota T, Ogata Y, Sekimizu K, Katayama
542 T. 2004. *DiaA*, a novel DnaA-binding protein, ensures the timely initiation of *Escherichia*
543 *coli* chromosome replication. J Biol Chem 279:45546-55.
544 42. Kato J, Katayama T. 2001. Hda, a novel DnaA-related protein, regulates the replication
545 cycle in *Escherichia coli*. EMBO J 20:4253-62.

546 43. Taghbalout A, Landoulsi A, Kern R, Yamazoe M, Hiraga S, Holland B, Kohiyama M,
547 Malki A. 2000. Competition between the replication initiator DnaA and the sequestration
548 factor SeqA for binding to the hemimethylated chromosomal origin of *E. coli in vitro*.
549 Genes to Cells 5:873-884.
550 44. Old IG, Margarita D, Saint Girons I. 1993. Unique genetic arrangement in the *dnaA* region
551 of the *Borrelia burgdorferi* linear chromosome: nucleotide sequence of the *dnaA* gene.
552 FEMS Microbiol Lett 111:109-14.
553 45. Fujikawa N, Kurumizaka H, Nureki O, Terada T, Shirouzu M, Katayama T, Yokoyama S.
554 2003. Structural basis of replication origin recognition by the DnaA protein. Nucleic Acids
555 Res 31:2077-86.
556 46. Barbour AG. 1984. Isolation and cultivation of Lyme disease spirochetes. Yale J Biol Med
557 57:521-5.
558 47. Savage CR, Jutras BL, Bestor A, Tilly K, Rosa PA, Tourand Y, Stewart PE, Brissette CA,
559 Stevenson B. 2018. *Borrelia burgdorferi* SpoVG DNA- and RNA-Binding Protein
560 Modulates the Physiology of the Lyme Disease Spirochete. J Bacteriol 200.
561 48. Sutton MD, Kaguni JM. 1997. Threonine 435 of *Escherichia coli* DnaA protein confers
562 sequence-specific DNA binding activity. J Biol Chem 272:23017-24.
563 49. Zawilak-Pawlik AM, Kois A, Zakrzewska-Czerwinska J. 2006. A simplified method for
564 purification of recombinant soluble DnaA proteins. Protein Expr Purif 48:126-33.
565 50. Qi X, Sun Y, Xiong S. 2015. A single freeze-thawing cycle for highly efficient
566 solubilization of inclusion body proteins and its refolding into bioactive form. Microb Cell
567 Fact 14:24.

568 51. Babb K, Bykowski T, Riley SP, Miller MC, Demoll E, Stevenson B. 2006. Borrelia
569 burgdorferi EbfC, a novel, chromosomally encoded protein, binds specific DNA sequences
570 adjacent to *erp* loci on the spirochete's resident cp32 prophages. J Bacteriol 188:4331-9.
571 52. Laniel MA, Béliveau A, Guérin SL. 2001. Electrophoretic mobility shift assays for the
572 analysis of DNA-protein interactions. Methods Mol Biol 148:13-30.
573 53. Arnold WK, Savage CR, Brissette CA, Seshu J, Livny J, Stevenson B. 2016. RNA-Seq of
574 *Borrelia burgdorferi* in Multiple Phases of Growth Reveals Insights into the Dynamics of
575 Gene Expression, Transcriptome Architecture, and Noncoding RNAs. PLoS One
576 11:e0164165.
577

Table 1. Subunits of DNA Polymerase III Holoenzyme

Subunit	Function	*E. coli*	*B. burgdorferi*	*T. pallidum*	*L. interrogans*
DnaE, α	Polymerase activity	B0184	BB0579	TP0669	LIC10222
DnaN, β	DNA clamp; locks Pol III to DNA to increase processivity	B3701	BB0438	TP0002	LIC10002
DnaQ, ε	3' → 5' exonuclease activity	B0215	–	TP0643	–
DnaX, τ and γ	Dimerize core enzymes (τ); clamp loader (γ)	B0470	BB0461	TP1005	LIC13474
HolA, δ	Clamp opener	B0640	BB0455	TP0588	–
HolB, δ'	Clamp loader	B1099	–	–	LIC13497
HolC, χ	Interact with SSB	B4259	–	–	–
HolD, Ψ	Stabilize γ and χ interaction	B4372	–	–	–
HolE, θ	Proof-reading activity	B1842	–	–	–

Dashes (–) indicate the organism lacks an identifiable homolog.

578
579
580
581

582 **Figure Legends.**

583 **Figure 1.** The *dnaX-ebfC* operon and its 5' UTR. (A) The *B. burgdorferi dnaX-ebfC* locus is
584 located downstream of genes for two tRNAs and the RNA component of the signal recognition
585 particle (SRP). (B) The predicted promoter (Softberry, BPROM) of the *dnaX-ebfC* operon is just
586 within the end of the *srp* gene. The 179 nt 5' UTR contains a hypothesized DnaA-box (A), and
587 two EbfC binding motifs. The region labeled B is the sequence DnaA was also found to bind (*see*
588 *below*).

589

590 **Figure 2.** Interactions of DnaA at the *dnaX-ebfC* 5' UTR DNA and assessment of effects of ATP
591 and ADP. Electrophoretic mobility shift assays (EMSAs) were conducted with a fluorescent 186-
592 mer DNA probe (100 nM) that consists of the *dnaX-ebfC* 5' UTR. Representative EMSAs with
593 0.050, 0.102, 0.206, 0.419, 0.851, 1.728, 3.509, 7.126 and 14.5 μM of recombinant GST-DnaA
594 with either 1 mM (A) ATP or (B) ADP. The first lanes contain the DNA probe only. (C) EMSA
595 with 0.625, 1.25, 2.5, and 5 μM recombinant GST demonstrates that the observed GST-DnaA
596 binding is not due to the fusion partner. (D-F) Apparent dissociation constant (K_D^{app}) measurements
597 of GST-DnaA-probe interactions with ATP or ADP. Plots show the K_D^{app} calculated using the
598 densitometric data from triplicate EMSAs. The average K_D^{app} for ATP reactions is 1141 nM and
599 737.7 nM for ADP. The difference in GST-DnaA-probe binding between the ATP and ADP
600 reactions was not statistically significant ($p = 0.9835$, unpaired student's t-test).

601

602 **Figure 3.** Identification of DnaA binding sites within the *dnaX-ebfC* 5' UTR DNA. (A) Schematic
603 of the 186-mer *dnaX-ebfC* 5' UTR DNA probe and the seven overlapping 40-mer DNA
604 competitors. Hypothesized DnaA-box is labeled A. The region where DnaA was also found to

605 bind is labeled B. (B) Horizontal EMSA with a polyacrylamide TBE gel using 100 nM DNA
606 probe, GST-DnaA, ATP, and different DNA competitors. Lane 1: probe only. Lanes 2-4: probe
607 with 1.125, 2.25, and 4.5 μM GST-DnaA. Lanes 5-11: probe with 4.5 μM GST-DnaA and 10-
608 molar excess of competitor DNAs (C1-C7). Lane 12: probe with 4.5 μM GST-DnaA and 10-molar
609 excess of DNA amplified from pCR2.1 containing the *dnaX-ebfC* 5'UTR (Positive control, PC).
610 Lane 13: probe with 4.5 μM GST-DnaA and 10-molar excess of DNA amplified from the empty
611 pCR2.1 (Negative control, NC). The asterisk marks the probe-protein complex. The black line
612 indicates the removal of extraneous lanes from the same gel.
613
614 **Figure 4.** Interactions of EbfC with the *dnaX-ebfC* 5' UTR DNA and RNA. (A-C) EMSAs with
615 100 nM labeled DNA probes, 2.5 ng/μl poly dI-dC, and either 3.75, 7.5, 15, and 30 μM
616 recombinant EbfC. Lane 1 for each panel is probe only. (A) 186-mer DNA probe of the *dnaX-ebfC*
617 5' UTR. (B) 30-mer DNA probe from the *dnaX-ebfC* 5' UTR with the consensus EbfC motif. (C)
618 30-mer DNA probe from the *dnaX-ebfC* 5' UTR with the partial EbfC motif. (D) Predicted RNA
619 fold structure of the 179 nt 5' UTR of *dnaX-ebfC* (RNAfold, http://rna.tbi.univie.ac.at/cgi-
620 bin/RNAWebSuite/RNAfold.cgi). The consensus EbfC binding motif is predicted to be part of a
621 stem-loop, and the partial EbfC binding motif is within a knot. (E) EMSA with 20 nM EbfC a 30-
622 mer Alexa 647 RNA probe containing the consensus EbfC binding motif from the *dnaX-ebfC* 5'
623 UTR and recombinant EbfC. Lane 1: probe only. Lanes 2-4: probe with 5, 10 and 15 μm EbfC.
624 Lane 5: probe with 1 μM competitor *flaB* RNA, and 15 μM EbfC. Lane 6: probe with 1 μM
625 competitor *dnaX-ebfC* RNA. The lower-order complex is indicated by one asterisk (*), and the
626 higher-order complex by two asterisks (**). All lanes are from the same gel, with the black line
627 indicating the removal of extraneous lanes.

628

629 **Figure 5.** Interaction of DnaA and EbfC at the *dnaX-ebfC* 5' UTR DNA. (A) EMSA using the
630 *dnaX-ebfC* probe with constant EbfC concentration of 10 μM and 0.078, 0.156, 0.312, 0.625, 1.25,
631 and 2.50 μM of GST-DnaA. Reaction A is EbfC only with the probe. Reactions B-G have an
632 increasing concentration of GST-DnaA and constant EbfC concentration. The first eight lanes
633 include 1 mM ATP, and the last seven include 1 mM ADP. (B) Graph of the percent free DNA for
634 each reaction as determined by densitometry. For both ATP and ADP conditions, free DNA
635 increased (reaction D) at lower concentrations of added GST-DnaA. At the highest GST-DnaA
636 concentrations, free DNA decreased.

637

638 **Figure 6.** The effects of purified recombinant protein on *dnaX-ebfC in vitro* expression. Reactions
639 used ~65 nM linear DNA containing 247 bp upstream of the *dnaX* start codon fused to *gfp*. GST-
640 DnaA, EbfC, or GST were added at final concentrations of 1 μM. Reporter GFP levels were
641 quantified by ELISA and are reported as mean absorbances from triplicate reactions. The error
642 bars indicate the standard error of the mean (SEM). Asterisks (****) indicate a statistically
643 significant ($p < 0.001$) difference relative to the template-only reaction. GST served as a control
644 to demonstrate the specific activity of the recombinant proteins. NTC = no template control.

645

646 **Figure 7.** EMSAs with PCR amplified probes containing the intergenic regions 5' of *dnaA* and the
647 DNA pol III HE genes. (A) Schematic of the loci subject to EMSA analysis. Predicted DnaA-
648 boxes are indicated by red rectangles. Mapped DnaA-boxes are indicated by purple rectangles.
649 Each EMSA reaction (B-E) includes 100 nM probe, 2.5 ng/μl poly dI-dC, and either 0.56, 1.125,
650 2.25, and 4.5 μM GST-DnaA. The first lane for each EMSA is probe only. The first five lanes of

651 each panel included 1 mM ATP, and the last five included 1 mM ADP. (B) Probe containing the
652 *oriC/dnaA-dnaN* intergenic region. (C) Probe containing the intergenic region of *gyrB-dnaA*. (D)
653 Probe containing the intergenic region 5' of *dnaE*. (E) Probe containing the intergenic region 5' of
654 *holA*.
655
656 **Figure 8.** Relative affinities of DnaA for labeled *oriC* probe in comparison with other loci.
657 Competitive EMSA using a final labeled *oriC* probe concentration of 100 nM for each lane. Lanes
658 2-4 have increasing concentrations of 1.125, 2.25, and 4.5 μM GST-DnaA, and lanes 5-10 have
659 constant levels of 4.5 μM GST-DnaA. Competitor DNAs were amplified using unlabeled M13
660 Forward and Reverse primers from TA constructs, and added at 10-times molar excess to reactions
661 relative to the *oriC* probe (lanes 6-10).
662
663 **Figure 9.** Tracking DNA Pol III HE gene expression changes during growth phases. **(A-F)** The
664 cell density of *B. burgdorferi* (left *y*-axes) was measured every 24 h, and the relative transcript
665 levels (right *y*-axes) were analyzed every 48 h. The fold expression of transcript was calculated by
666 normalization to the constitutive *ftsK* gene and reported as the average of triplicate reactions. The
667 error bars indicate the SEM.
668
669 **Figure 10.** Diagram of experimentally-confirmed and hypothesized effects of DnaA on *B.*
670 *burgdorferi* protein expression. Green arrows indicate positive effects, red arrows indicate
671 negative effects, and black arrows indicate predicted effects. DnaA positively influences
672 expression of both DnaX and EbfC. EbfC counteracts the effect of DnaA on the *dnaX-ebfC* operon,
673 acts as an anti-repressor to stimulate transcription of *erp* operons, and also affects expression of

674 numerous other transcripts. DnaA binds over the *bpuR* promoter and is hypothesized to repress
675 transcription of that gene, while BpuR has been demonstrated to repress its own translation,
676 enhance repression of *erp* operons, and affect expression of several other borrelial proteins. DnaA
677 also binds to its own promoter region, as well as those of *dnaE, dnaN, gyrB,* and *holA*, and is
678 hypothesized to affect expression of those operons.
679

680 **Supplementary Material.**

681 **Supplemental Figure.** Top: Alignment of slipped-strand region of *E. coli* (Ec) *dnaX* gene with
682 those of *B. burgdorferi* (Bb) and the spirochetes *Treponema pallidum* (Tp) and *Leptospira*
683 *interrogans* (Li). The *dnaX* gene and protein sequences were taken from the type strains of *E. coli*
684 (NC_000913), *B. burgdorferi* (NC_001318), *T. pallidum* (NC_000919), and *L. interrogans*
685 (NZ_CP02414). The *E. coli dnaX* gene sequence was annotated to show the Shine-Dalgarno (RBS)
686 sequence, slippery sequence, and frameshift stop codon (16). Sequence alignments were
687 performed on Geneious software using Clustal Omega. Bottom: Identities of the *dnaX* genes and
688 DnaX proteins of *E. coli* (Ec), *B. burgdorferi* (Bb), *T. pallidum* (Tp), and *L. interrogans* (Li).

689

690 **Supplemental Table.** Oligonucleotides used in these studies

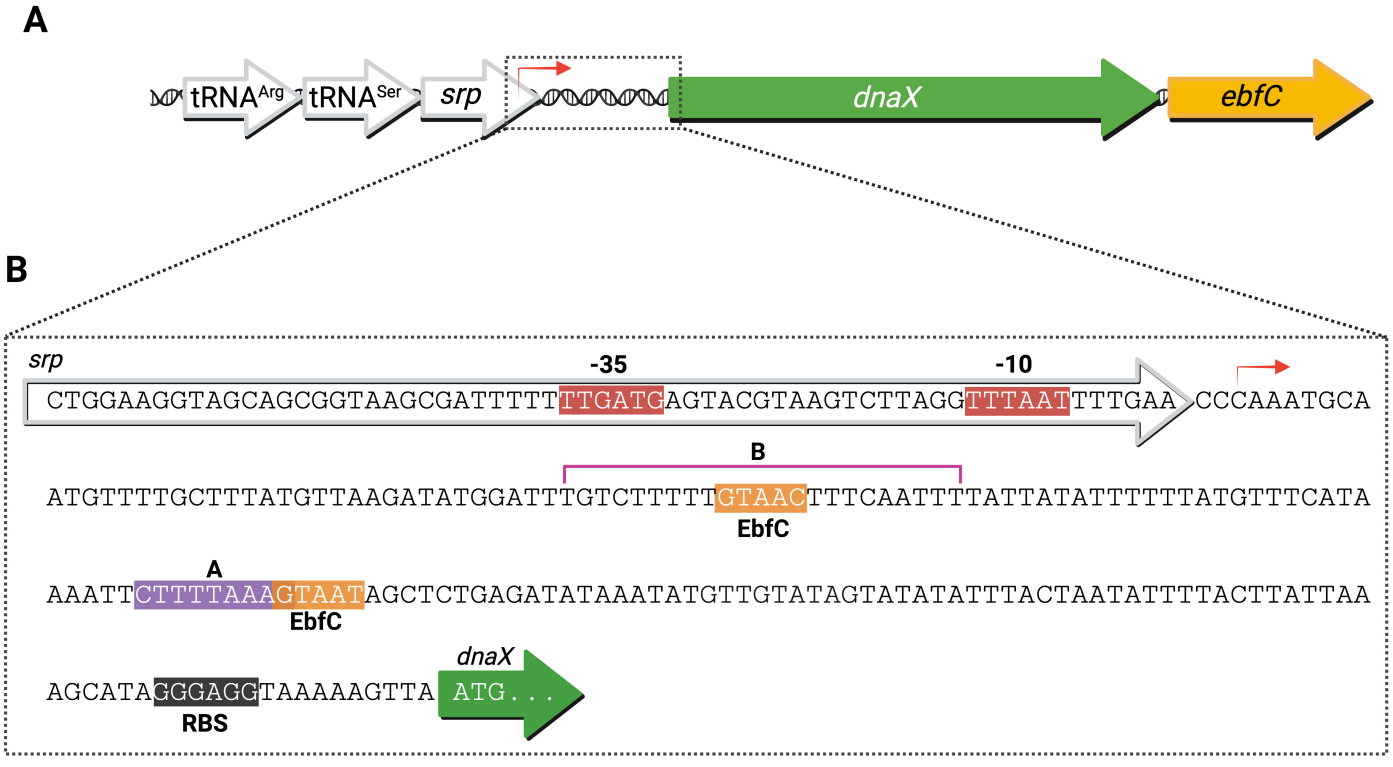
A
tRNA^Arg
tRNA^Ser
srp
dnaX
ebfC
B
srp
-35
-10
CTGGAAGGTAGCAGCGGTAAGCGATTTTTTTGATCAGTACGTAAGTCTTAGGTTTAATTTTGAACCCAAATGCA
B
ATGTTTTGCTTTATGTTAAGATATGGATTTGTCTTTTTGTAACTTTCAATTTTATTATATTTTTTATGTTTCATA
EbfC
A
AAATTCTTTTAAAGTAATAGCTCTGAGATATAAATATGTTGTATAGTATATATTTACTAATATTTTACTTATTAA
EbfC
dnaX
AGCATAGGGAGGTAAAAAGTTA ATG...
RBS

Figure 1

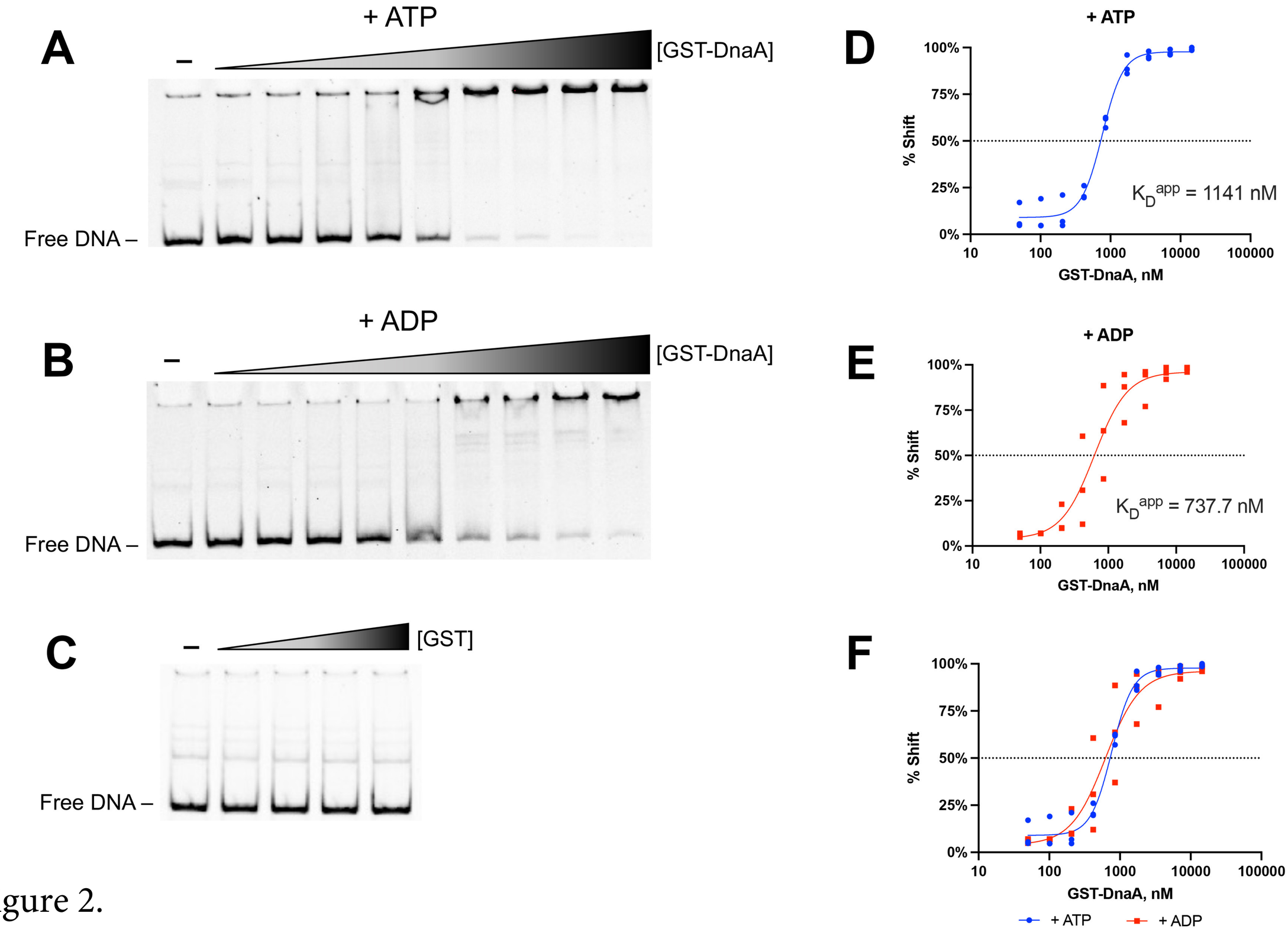
A
+ ATP
–
[GST-DnaA]
Free DNA –
B
+ ADP
–
[GST-DnaA]
Free DNA –
C
–
[GST]
Free DNA –
D
+ ATP
% Shift
100%
75%
50%
25%
0%
10
100
1000
10000
100000
GST-DnaA, nM
K_D^{app} = 1141 nM
E
+ ADP
% Shift
100%
75%
50%
25%
0%
10
100
1000
10000
100000
GST-DnaA, nM
K_D^{app} = 737.7 nM
F
% Shift
100%
75%
50%
25%
0%
10
100
1000
10000
100000
GST-DnaA, nM
+ ATP
+ ADP

Figure 2.

A

***dnaX-ebfC* 5' UTR DNA Probe**

B

A

GGTTTAATTTTGAACCCAAATGCAATGTTTTGCTTTATGTTAAGATATGGATTTGTCTTTTTGTAACTTTCAATTTTATTATATTTTTTATGTTTCATAAAATTCTTTTAAAGTAATAGCTCTGAGATATAAATATGTTGTATAGTATATATTTACTAATATTTTACTTATTAAAGCATAGGGAGG

Competitor 1

TTTAATTTTGAACCCAAATGCAATGTTTTGCTTTATGTTAAGATAT

Competitor 3

TCATAAAATTCTTTTAAAGTAATAGCTCTGAGATATAAATATGT

Competitor 2

GGATTTGTCTTTTTGTAACTTTCAATTTTATTATATTTTTTATGTT

Competitor 4

TGTATAGTATATATTTACTAATATTTTACTTATTAAAGCATAGGG

Competitor 5

AATGCAATGTTTTGCTTTATGTTAAGATATGGATTTGTCTTTTT

Competitor 6

TTTCAATTTTATTATATTTTTTATGTTTCATAAAATTCTTTTAAA

Competitor 7

AGCTCTGAGATATAAATATGTTGTATAGTATATATTTACTAATAT

B

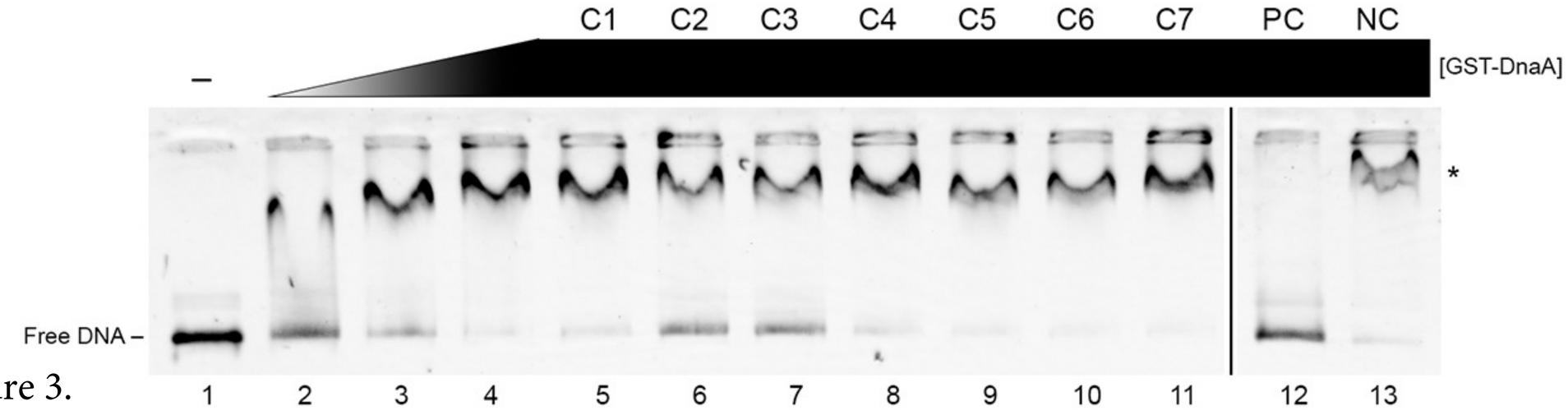

Figure 3.

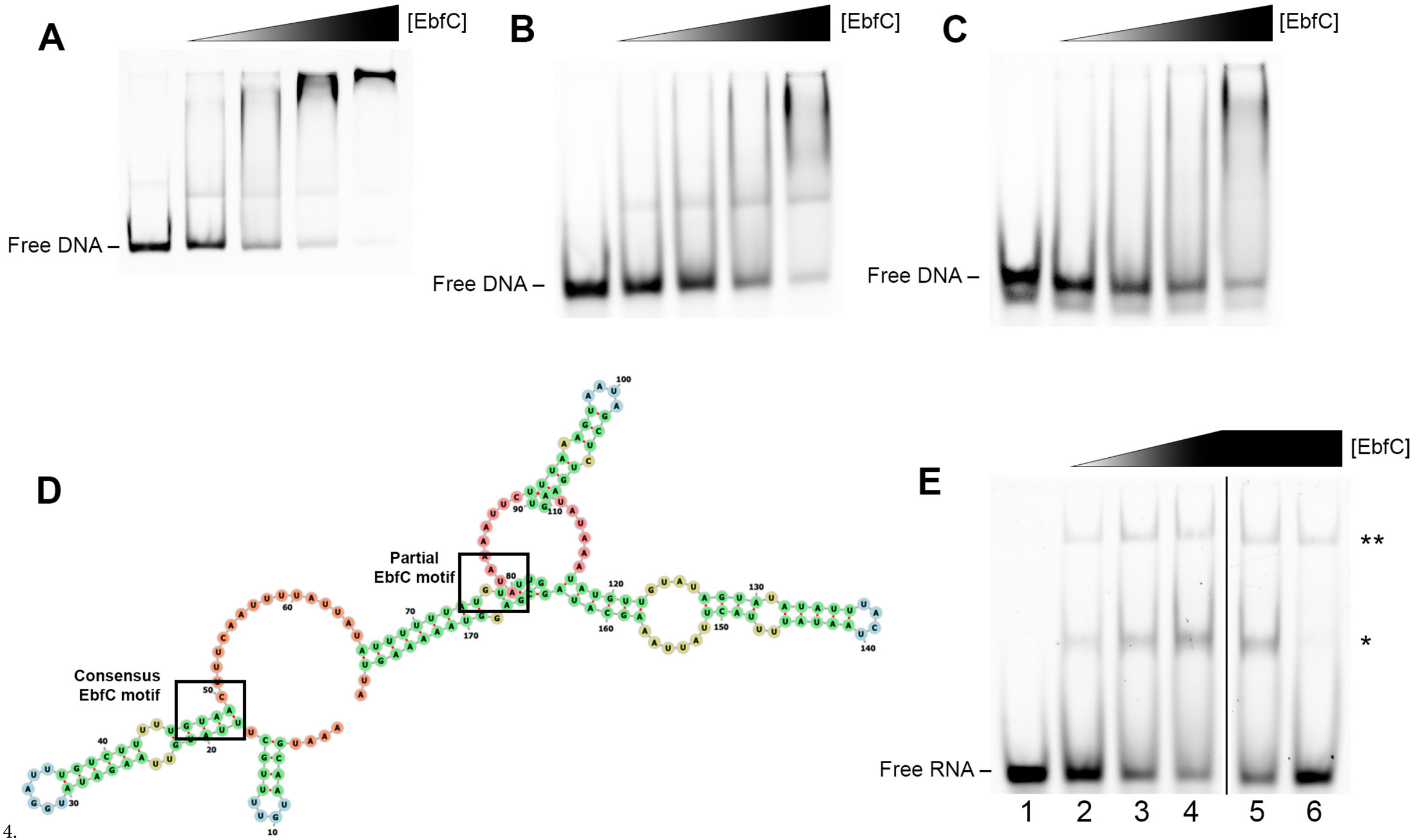
A
[EbfC]
Free DNA –
B
[EbfC]
Free DNA –
C
[EbfC]
Free DNA –
D
Partial
EbfC motif
Consensus
EbfC motif
E
[EbfC]
**
*
Free RNA –
1
2
3
4
5
6

Figure 4.

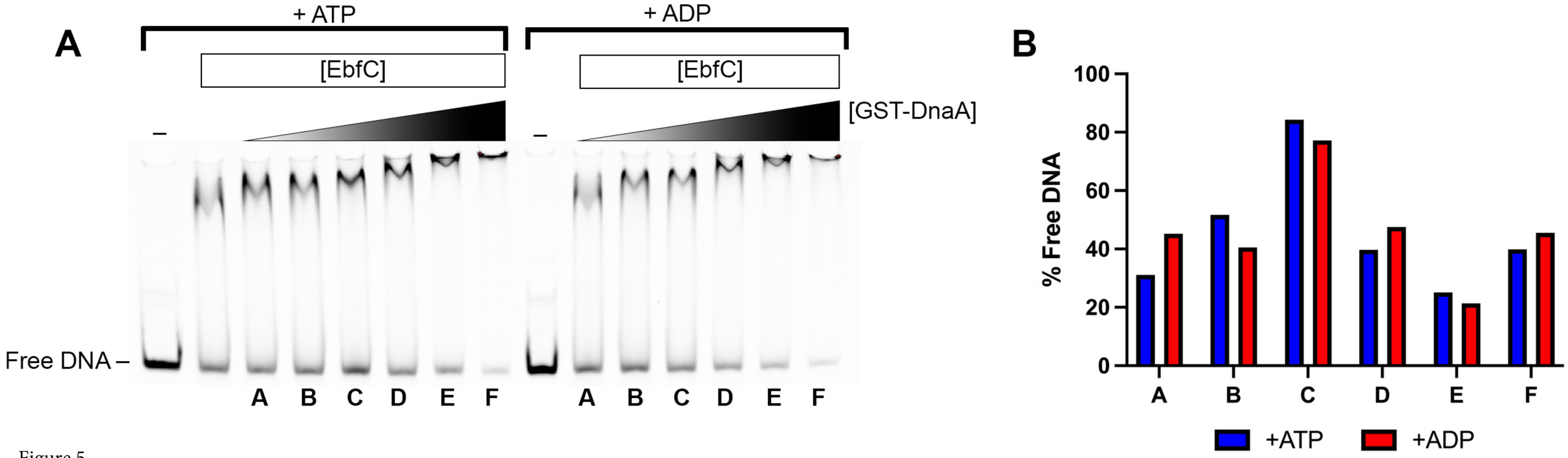
A
+ ATP
+ ADP
[EbfC]
[EbfC]
[GST-DnaA]
–
–
Free DNA –
A B C D E F
A B C D E F
B
% Free DNA
100
80
60
40
20
0
A B C D E F
+ATP
+ADP

Figure 5.

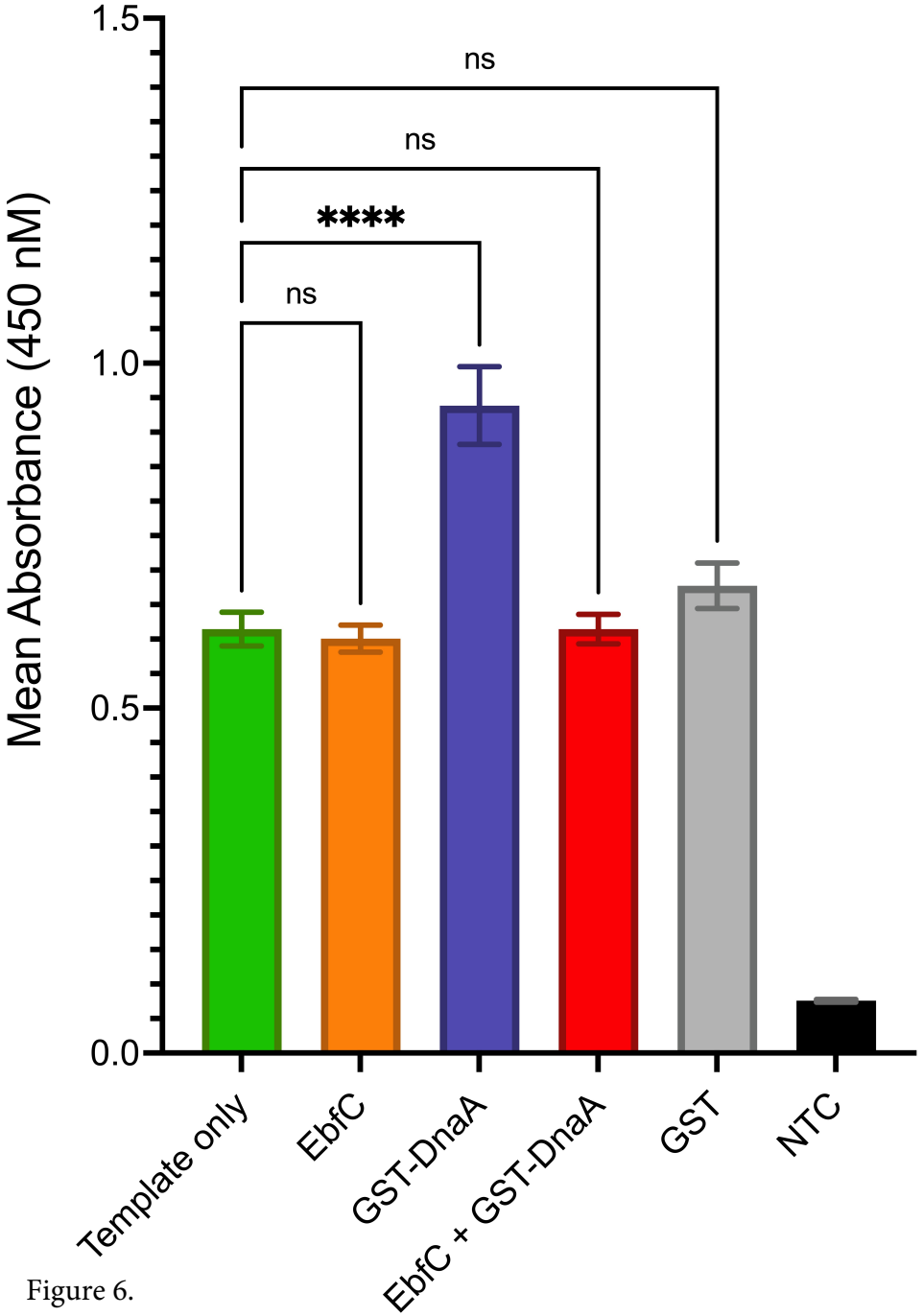
1.5
1.0
0.5
0.0
Mean Absorbance (450 nM)
ns
ns
****
ns
Template only
EbfC
GST-DnaA
EbfC + GST-DnaA
GST
NTC

Figure 6.

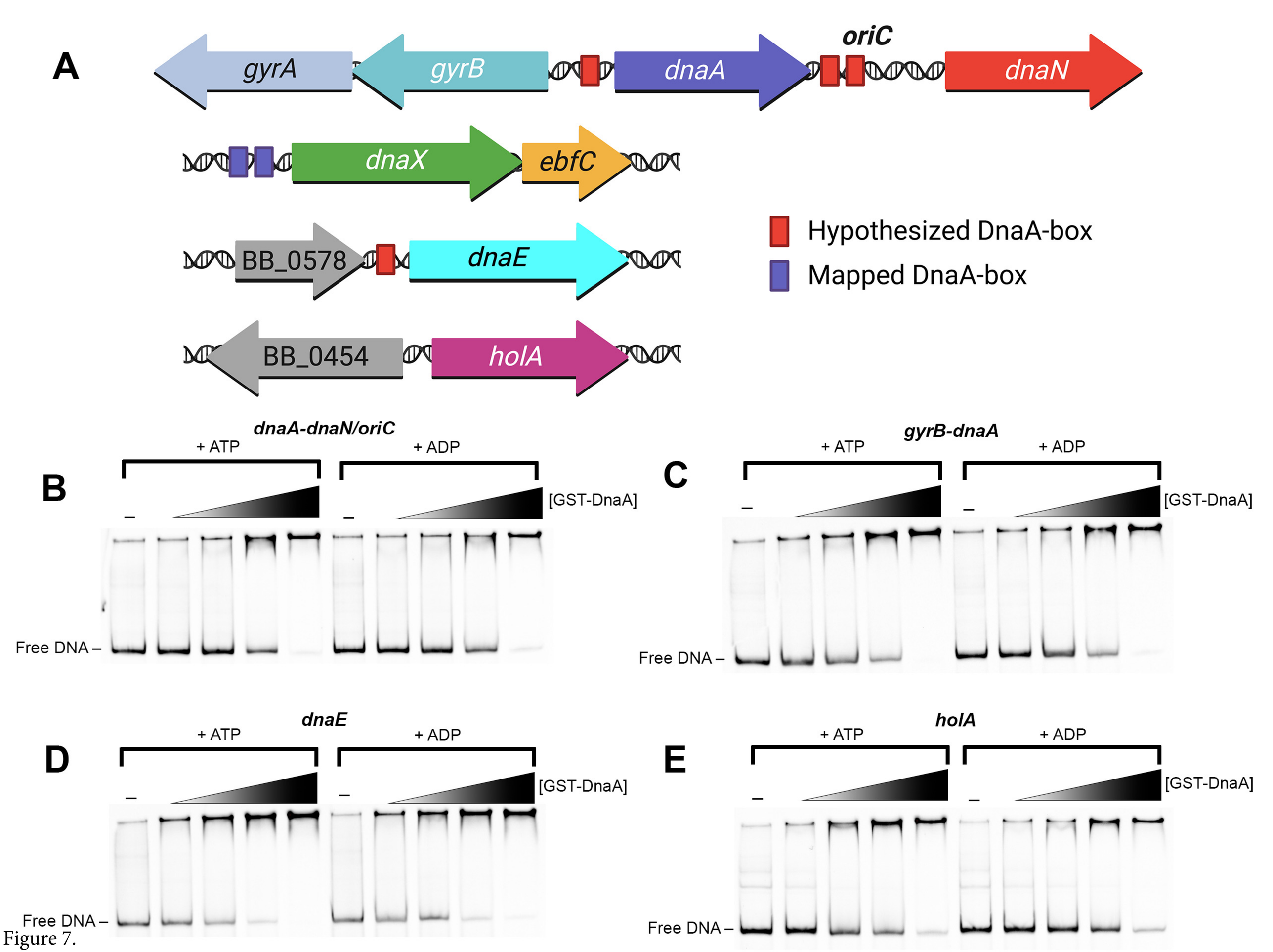
A
gyrA
gyrB
dnaA
oriC
dnaN
dnaX
ebfC
BB_0578
dnaE
BB_0454
holA
Hypothesized DnaA-box
Mapped DnaA-box
B
dnaA-dnaN/oriC
+ ATP
+ ADP
[GST-DnaA]
Free DNA
C
gyrB-dnaA
+ ATP
+ ADP
[GST-DnaA]
Free DNA
D
dnaE
+ ATP
+ ADP
[GST-DnaA]
Free DNA
E
holA
+ ATP
+ ADP
[GST-DnaA]
Free DNA

Figure 7.

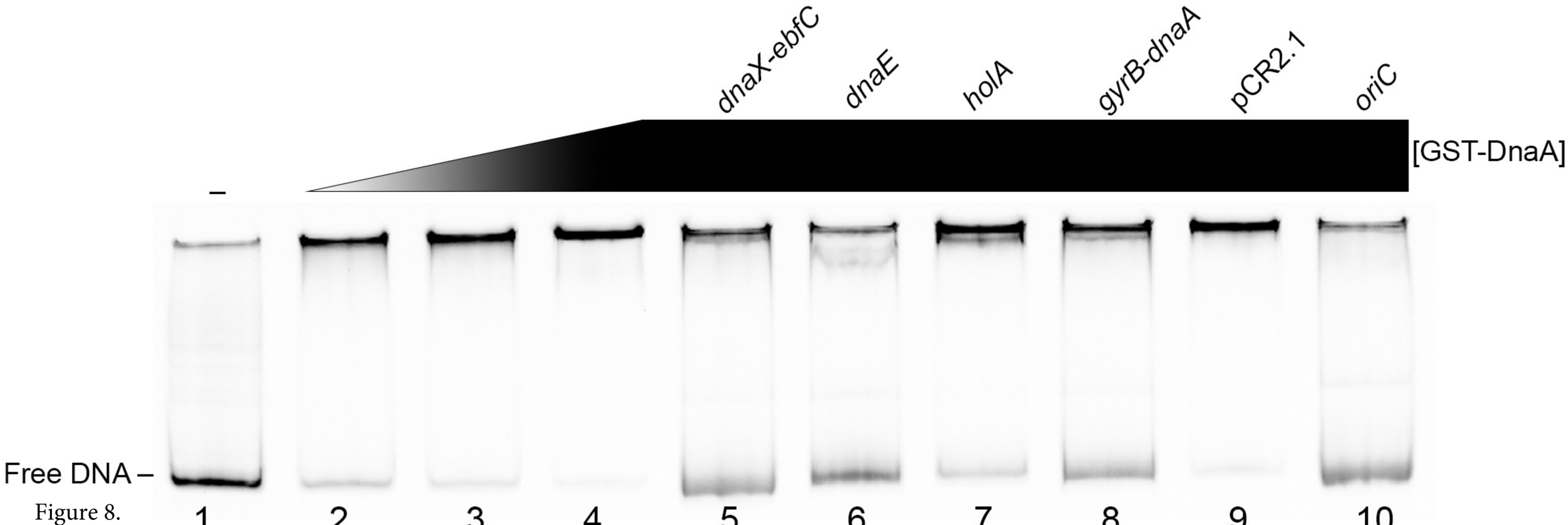
dnaX-ebfC
dnaE
holA
gyrB-dnaA
pCR2.1
oriC
[GST-DnaA]
–
Free DNA –
1
2
3
4
5
6
7
8
9
10

Figure 8.

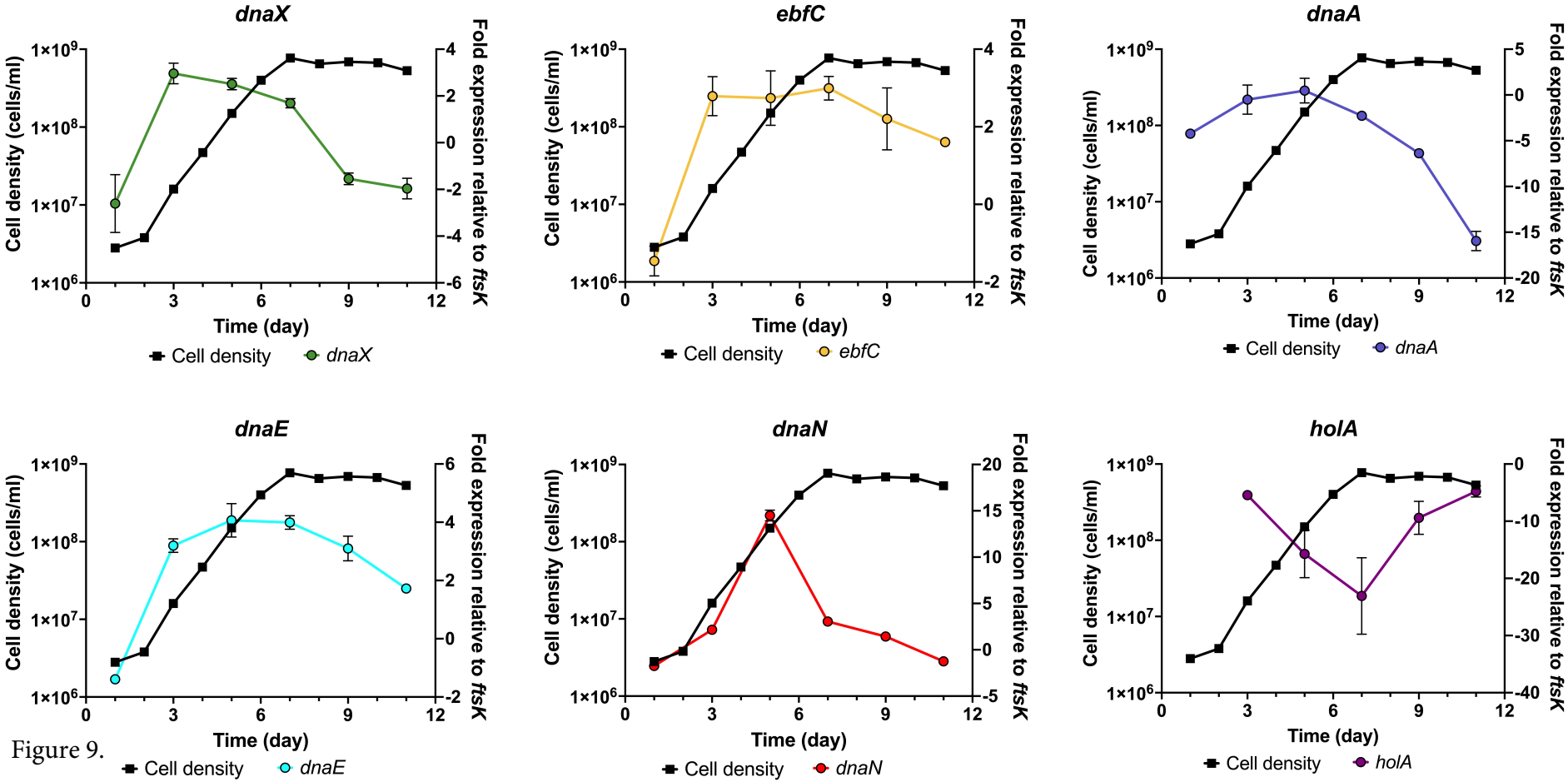
dnaX
ebfC
dnaA
dnaE
dnaN
holA
Cell density (cells/ml)
Fold expression relative to ftsK
Time (day)
Cell density
dnaX
ebfC
dnaA
dnaE
dnaN
holA

Figure 9.

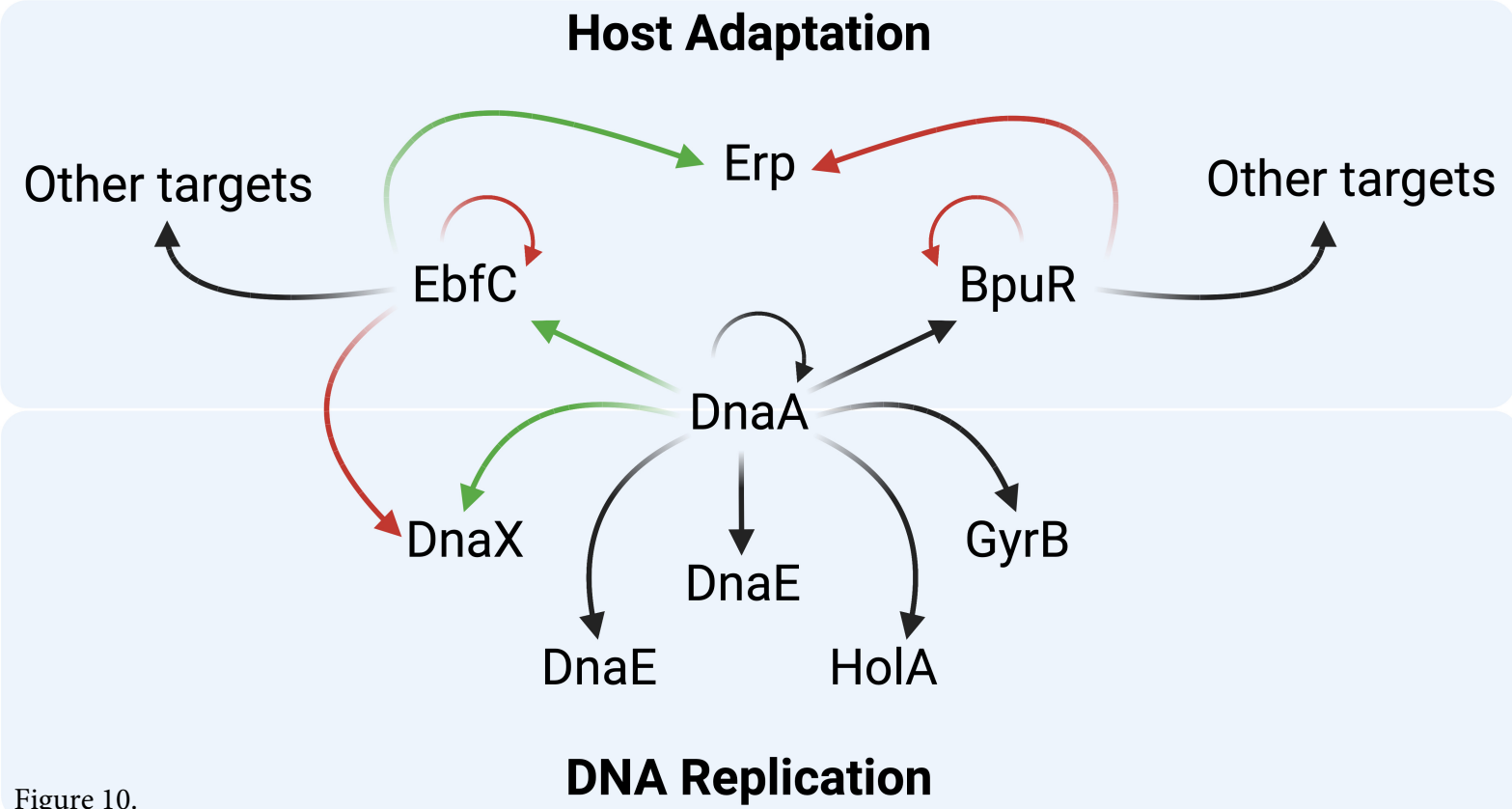
Host Adaptation
Other targets
Erp
Other targets
EbfC
BpuR
DnaA
DnaX
DnaE
GyrB
DnaE
HolA
DNA Replication

Figure 10.